Pertanika J. Sci. & Technol. 33 (S2): 13 - 25 (2025)

PERTANIKA JOURNALS

SCIENCE & TECHNOLOGY

Journal homepage: http://www.pertanika.upm.edu.my/

Numerical Analysis of the Load-carrying Capacity of Built-up Columns with Damaged or Missing Lacing Bars

Toshikazu Takai[1]*, Taiyo Furuichi[2], Takao Miyoshi[3], Kaname Iwatsubo[4], Kazuya Tamada[5] and Kenta Morimoto[6]

[1]Department of Civil and Architectural Engineering, Faculty of Engineering, Kyushu Institute of Technology, Kitakyushu 804-8550, Japan
[2]Former student, Department of Civil Engineering and Architecture, School of Engineering, Kyushu Institute of Technology, Kitakyushu 804-8550, Japan
[3]Department of Civil Engineering, National Institute of Technology (KOSEN), Akashi College, Akashi 674-8501, Japan
[4]Production System Engineering Course, National Institute of Technology (KOSEN), Kumamoto College, Yatsushiro 866-8501, Japan
[5]Department of Civil Engineering and Architecture, National Institute of Technology (KOSEN), Maizuru College, Maizuru 625-8511, Japan
[6]Department of Engineering, Graduate School of Engineering, Kyushu Institute of Technology, Kitakyushu 804-8550, Japan

ABSTRACT

Built-up columns with lacing bars are commonly used in old bridges. Typically, these columns consist of shaped steel members connected by riveted lacing bars. This design held the advantage of reducing steel usage, thereby lowering costs. However, these techniques have become outdated. Nevertheless, structures constructed using these methods persist today. Over time, some of these columns have experienced component loss because of ageing, damage, or corrosion. This study uses finite element analysis to determine the load-carrying capacity of built-up columns with lacing bars subjected to compressive forces. The results indicate that the loss of some lacing bars results in a 2% reduction in load-carrying capacity, while the loss of both lacing bars and rivets leads to a 5% reduction. Though the reduction may appear marginal, the presence or absence of lacing bars and rivets becomes a significant consideration in estimating the remaining load-carrying capacity. The results of this study have implications with respect to the ongoing use and maintenance of built-up columns with missing components, which has emerged as a critical concern.

Keywords: Buckling, built-up column, finite element analysis, lacing bar, riveted connection

ARTICLE INFO

Article history:
Received: 13 February 2024
Accepted: 18 October 2024
Published: 25 February 2025

DOI: https://doi.org/10.47836/pjst.33.S2.02

E-mail addresses:
takai@civil.kyutech.ac.jp (Toshikazu Takai)
furuichi.taiyo521@mail.kyutech.jp (Taiyo Furuichi)
miyoshi@akashi.ac.jp (Takao Miyoshi)
iwatsubo@kumamoto-nct.ac.jp (Kaname Iwatsubo)
tamada@maizuru-ct.ac.jp (Kazuya Tamada)
morimoto.kenta110@mail.kyutech.jp (Kenta Morimoto)
* Corresponding author

ISSN: 0128-7680
e-ISSN: 2231-8526

INTRODUCTION

Built-up columns with lacing bars are commonly used in old bridges, as shown in Figure 1. These columns typically consist of channel-shaped steel members and lacing bars. The lacing bars are connected to the channel-shaped steel with a rivet, reducing the required steel and construction costs. Miyoshi (2021a) investigated previous Japanese specifications for highway bridges. Regulations on built-up columns were deleted from the Japanese highway bridge specifications and revised in 1980 (JRA, 1980). Similarly, regulations on riveted connections were deleted from the Japanese specifications for highway bridges and were revised in 1990 (JRA, 1990). These techniques are currently old; however, structures that utilise these techniques still exist. As shown in Figure 1, some columns lose their components because of ageing, damage, or corrosion. The load-carrying capacity of a column that has lost some components is important for maintaining and continuing to use these structures. Therefore, the load-carrying capacity of the columns must be determined.

Previous studies investigated the mechanical behaviours of a plate with a corroded surface, such as buckling load (Sadovsky & Drdacky, 2001) and ultimate shear strength (Paik et al., 2004). Beaulieu et al. (2010) experimentally studied the compressive strength of corroded steel angles. The capacity of the angle was compared with design codes. Hisazumi et al. (2018) investigated the buckling load of corroded steel channels and angle members by considering the local buckling behaviour. Thus, the mechanical behaviour of corroded steel members has been investigated in some studies. A built-up column contains several components. The interaction of the components exhibits mechanical behaviour, thereby impacting the corrosion complex. However, studies on the mechanical behaviour of corroded built-up columns are lacking.

Although the column missing lacing bars or rivets are present, the load-carrying capacity of such column is unknown. The authors have previously conducted studies

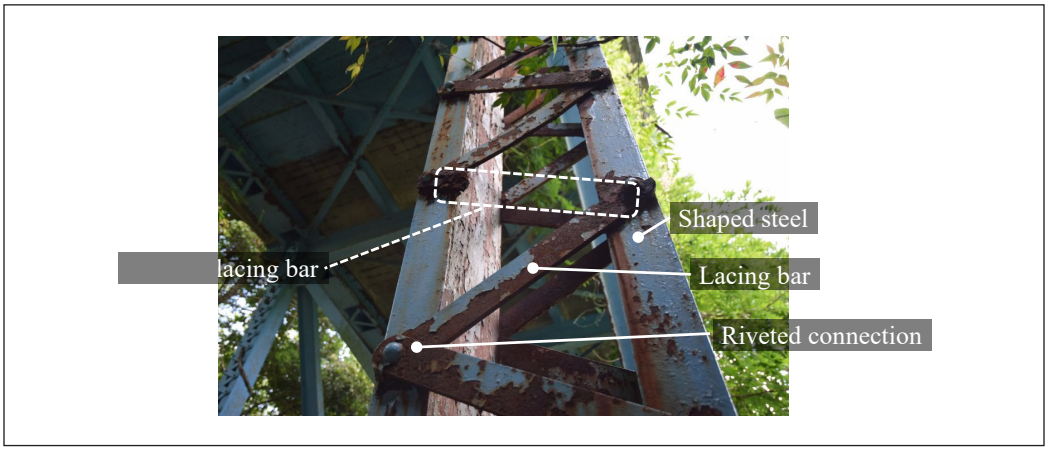

Figure 1. A built-up column. The column appears old and is missing a lacing bar

to determine the load-carrying capacity of built-up columns with lacing bars, both experimentally (Miyoshi et al., 2021b, 2021c, 2022; Nakakita et al., 2021) and numerically (Iwatsubo et al., 2020a, 2020b; Kojima & Takai, 2021; Miyoshi et al., 2022; Nakakita et al., 2022). However, the numerical evaluation was conducted by modelling the riveted connections (between the shaped steel and lacing bars) using simple models with limitations. Therefore, the detailed influence of missing rivets and lacing bars, considering the behaviour of the area around the rivet holes, on a column's load-carrying capacity was not evaluated. This study investigated the necessity of modelling riveted connections using finite element analysis. Moreover, the load-carrying capacity of columns, with lacing bars and rivets missing, was investigated.

NUMERICAL MODELLING OF THE AREA AROUND RIVETED CONNECTIONS

Methods

The load-carrying capacity analysis of the channel-shaped steel of a built-up column examined the modelling in the area around the riveted connections. The numerical analysis was conducted using Abaqus/Standard 6.13. Figure 2 depicts an outline of the numerical model. Shaped steel was integrated as a component of the built-up column. The thicknesses of the flange and web plates were 3.5 mm. A linearly reduced integration 8-node solid element was used. The length of each element was approximately 1.2 mm. The plate was divided into three elements along the thickness direction. The initial deflection and residual stress specifications illustrated in Figures 3 and 4 were applied to the model as initial imperfections. The shape of the initial deflection was sinusoidal, with an amplitude equal to

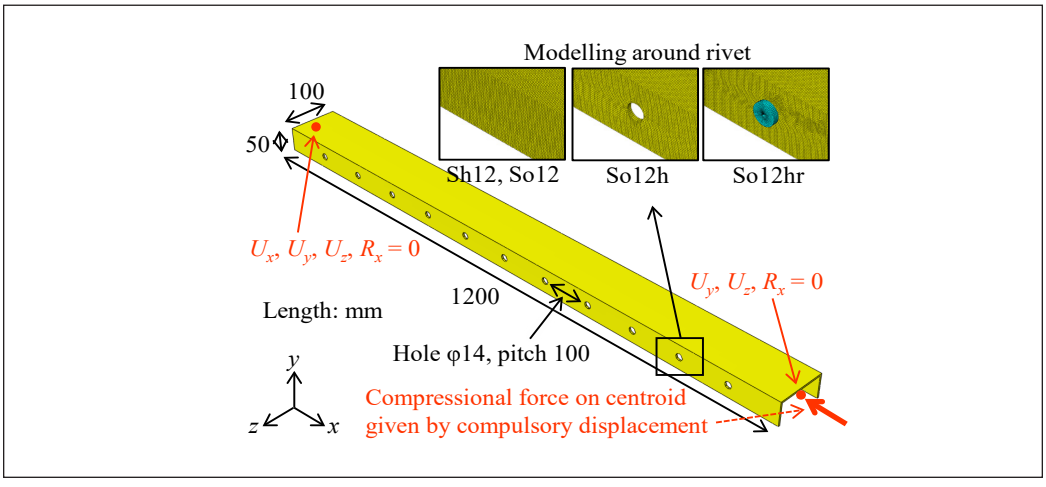

Figure 2. Outline of the numerical model. The centroid on one side of the column is fixed; the other is set to compulsory displacement to provide compressional force

the maximum fabrication tolerance of the steel members of highway bridges (JRA, 1990). The direction of initial deflection was determined using an eigenvalue buckling analysis conducted in advance. The residual stress was set considering the stress equilibrium in the cross-section (Iwatsubo et al., 2020a, 2020b). A compression load was applied to the column by the compulsory displacement of the centroid at the end of the column. The stress-strain relationship values are summarised in Table 1. These values assume the steel grade of SM490Y (JIS G 3106, 2020). The 200 000 N/mm^2 and 0.3 values were used for Young's modulus and Poisson's ratio, respectively. The material properties of the channel steel and the rivets were identical.

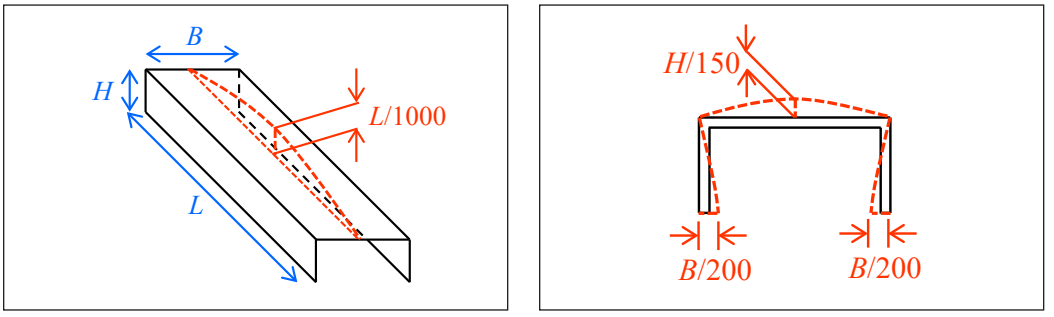

Figure 3. Initial deflection specifications. The shape of the deflection is sinusoidal, with an amplitude equal to the maximum fabrication tolerance of the steel members of highway bridges: (a) Whole length; and (b) Cross-section

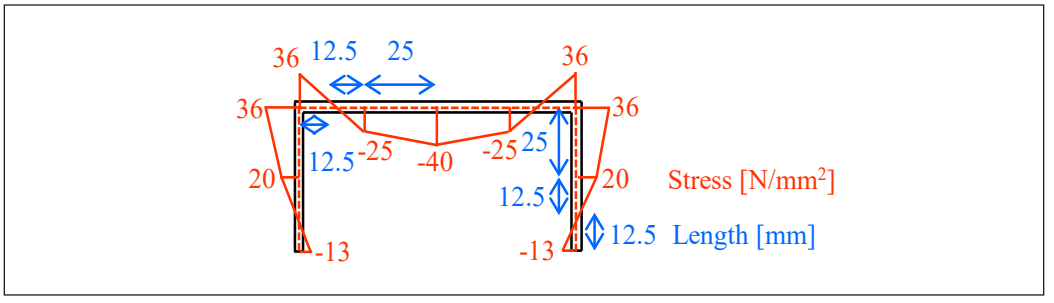

Figure 4. Residual stress specifications. The residual stress is set considering the stress equilibrium in the cross-section

Table 1
Stress-strain relationship values

	Nominal stress [N/mm^2]	Nominal strain	True stress [N/mm^2]	True strain
Yield point	355	0.0018	356	0.0018
Tensile strength	551	0.0996	606	0.0950

Investigated Cases

The analysed cases are summarised in Table 2. The shell and solid element cases were compared under identical conditions. These cases differed only in terms of element type. In comparison, the application of solid elements to the load-carrying capacity analysis of a compressional column was investigated; however, for a buckling analysis, a compressional column is typically modelled using shell elements. Solid elements are beneficial in stereographically modelling the details of riveted connections to replicate the contact between rivets and holes. The findings from this comparative investigation corroborate the application of the solid element model to the numerical analysis of load-carrying capacity involving buckling behaviour. Our study involved two distinct column lengths: (1) a 300 mm column referred to as a "stub column" and (2) a 1200 mm column designated as a "long column." The stub column exhibited a buckling load that exceeded the compressional yield load, determined by multiplying the yield point and cross-sectional area. In contrast, the long column did not surpass the compressional yield load in terms of its buckling load. A column with rivet holes and rivets was analysed for the solid element cases to determine the necessity of accurately modelling the riveted connections.

Table 2
Specifications of the investigated cases

Case name	Element type	Length [mm]	Rivet holes	Rivets
Sh3	Shell	300	Not modelled	Not modelled
So3	Solid	300	Not modelled	Not modelled
So3h	Solid	300	Modelled	Not modelled
So3hr	Solid	300	Modelled	Modelled
Sh12	Shell	1200	Not modelled	Not modelled
So12	Solid	1200	Not modelled	Not modelled
So12h	Solid	1200	Modelled	Not modelled
So12hr	Solid	1200	Modelled	Modelled

Results

Table 3 summarises the maximum load and corresponding displacement values for each case. The reduction value for each case is the percentage difference between the maximum load and that of the shell element case of the same length. The difference between the shell element cases Sh3 and Sh12 and the solid element cases So3 and So12 was less than 1%. However, the maximum load in the cases with rivet holes, So3h and So12h, was reduced by more than 15%. The reduction was significantly less for the cases with holes and rivets, that is, So3hr and So12hr. These values were approximately 3% lower than those of Sh3 or Sh12.

Figure 5 shows the obtained load-displacement curves. The vertical axis represents the dimensionless value *P/Py*, the ratio of the compressed load to the design yield load. The design yield load is obtained by multiplying the yield point by the cross-sectional area without rivet holes. The horizontal axis represents the dimensionless value *U/Uy*, the ratio of the displacement to the yield displacement. The yield displacement was obtained by multiplying the yield strain by the column length. The displacement was measured at the centroid-applied compulsory displacement at the end of the column. First, the load increased linearly in each case. The load increased linearly for the 300 mm length case, then gradually reached the maximum load. In contrast, for the 1200 mm cases, the load increased linearly and suddenly decreased.

Figure 6 shows the von Mises stress distribution at the maximum load. The distributions of shell element cases Sh3 and Sh12 were the same as those of solid element cases So3 and So12, respectively. For cases such as So3h and So12h, where rivet holes were used, stress concentration occurred around the rivet holes. The stress was lower than that in the cases So3 and So12 (without holes). In contrast, for cases So3hr and So12hr (holes with rivets), the stress distribution was approximately equal to So3 and So12, respectively, despite the stress in the rivets being significantly smaller.

Table 3
Maximum load and displacement results

Case name	P_{max} [kN]	Reduction* [%]	U_{Pmax} [mm]
Sh3	235	0.0	0.6
So3	234	-0.4	0.6
So3h	179	-23.8	0.7
So3hr	227	-3.4	0.6
Sh12	148	0.0	1.4
So12	147	-0.7	1.4
So12h	122	-17.6	1.2
So12hr	144	-2.7	1.3

*Reduction is the percentage difference between the maximum load and the shell element case of the same length

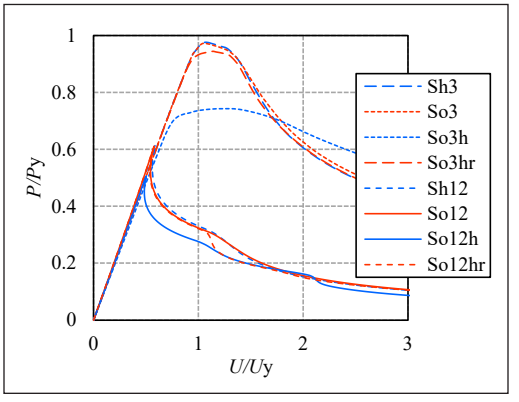

Figure 5. Load-displacement curves. The curves of the cases Sh3, So3, and So3hr are almost the same. While the cases Sh12, So12, and So12hr have almost the same curves. However, the maximum loads of the cases So3h and So12h are lower than those of the others

Discussion

Comparing Sh3 and So3, or Sh12 and So12, the obtained maximum load and load-displacement curves in Figure 5 were approximately equal. Similarly, the overall stress distributions were approximately equal, as shown in Figure 6. In previous studies, the numerical analysis of compressed columns, including buckling behaviour, has typically

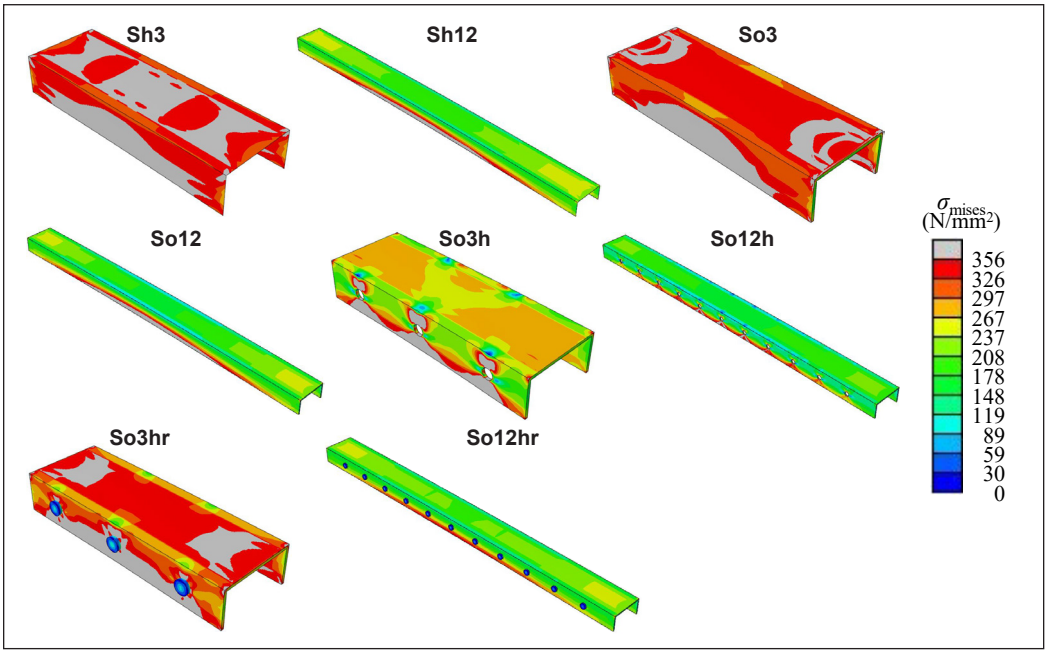

Figure 6. von Mises stress distribution at maximum load. The distributions of the cases Sh3, So3, and So3hr are almost the same. While the cases Sh12, So12, and So12hr have almost the same distributions. Stress concentration occurs around the rivet holes in cases So3h and So12h (with holes). In these cases, the stress is lower than that in So3 and So12 (without holes)

been conducted using shell elements. However, this result indicates that numerical analysis using solid elements yields results equal to shell elements. Hence, solid elements can be adapted to finite element analysis to evaluate a compressed column. Conveniently, applying solid elements enables us to replicate the contact between rivets and holes and evaluate the detailed behaviour of the riveted connection. Based on this result, a further evaluation of the detailed behaviour of the area around the riveted holes was conducted using solid element models.

As shown in Figure 5, the maximum loads of cases So3h and So12h (with rivet holes modelled) were lower than those of So3 and So12 (without holes modelled), respectively, because of the reduction in the net cross-sectional area owing to the rivet holes. The occasion of stress concentration by the holes, as shown in Figure 6, reduced the maximum load. However, by filling the hole with a rivet, that is, in cases So3hr and So12hr, the reduction in the maximum load was minimised because the contact between the rivet axis and the hole transmitted compressional forces. The stress concentration around the rivet holes decreased from So3h to So12h. The maximum loads of So3hr and So12hr were approximately equal or marginally less than those of So3 and So12, respectively. This result suggests that despite the maximum load being equal for both cases, modelling rivets and rivet holes is necessary to evaluate the detailed behaviour, including the area around the

rivet connection. Because the load-carrying capacity of the columns with missing lacing bars and rivets was unknown, the parametric study in the next section was performed.

COMPRESSIONAL BEHAVIOUR OF BUILT-UP COLUMN WITH MISSING LACING BARS

Methods

The built-up column was modelled based on previous studies (Iwatsubo et al., 2020a, 2020b). The column comprised two channel-shaped steel members and 24 lacing bars. The lacing bars were tightened using rivets. Figure 7 shows an outline of the numerical model. The column length was 900 mm. The channel steel had flange plates 50 mm wide and a web plate 100 mm wide. The thickness of the plate was 9 mm. The dimensions of the lacing bars were 170×20×4 mm. The diameter of the rivet holes was 14 mm. The hole pitch was 115.5 mm. The friction coefficient was 0.1. The model included initial imperfections: the initial deflection in Figure 8 and the residual stress in Figure 4. The direction of the initial deflection was determined using eigenvalue buckling analysis. The lengths of the

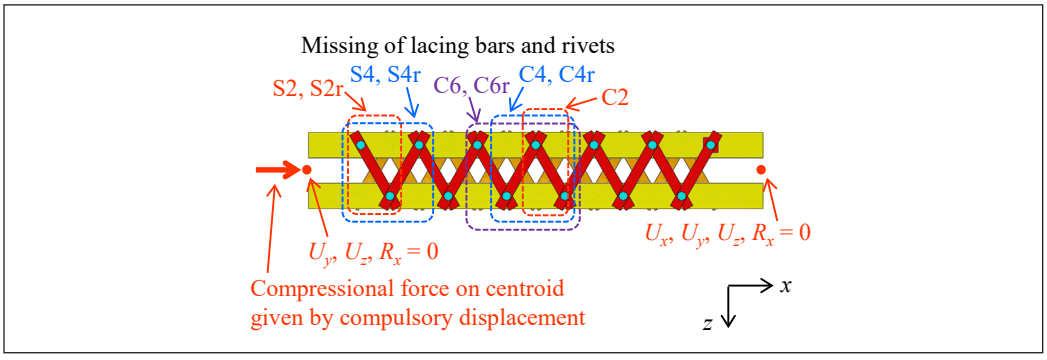

Figure 7. Outline of numerical model. The S-series cases are missing lacing bars near the sides of the column, whereas those of the C-series are missing lacing bars at the centre of the column

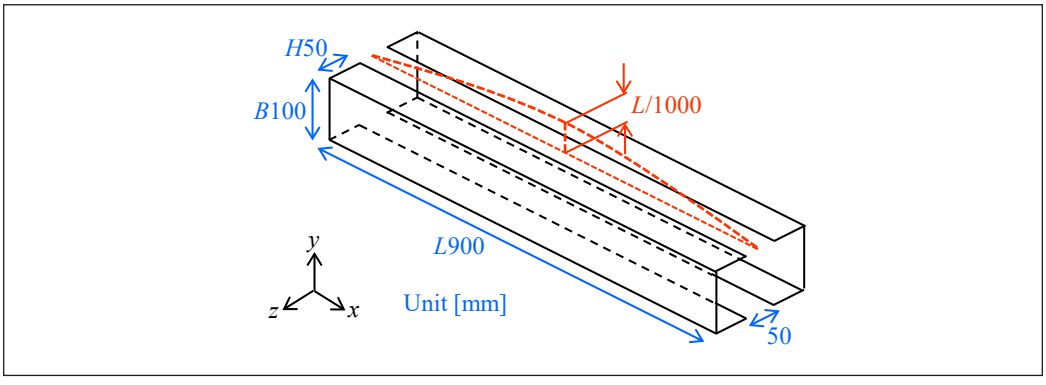

Figure 8. Initial deflection specifications. The deflection shape is sinusoidal, with an amplitude equal to the maximum fabrication tolerance of the steel members of highway bridges

solid elements were approximately 1.5 mm. The material properties are the same as those described in the previous section.

Investigated Cases

Table 4 summarises the analysed cases. N0 represents the normal case without any loss of lacing bars or rivets. The S-series cases lost lacing bars near the side ends of the column. The C-series cases lost lacing bars at the centre of the column. The cases with names including "r" lost not only lacing bars but also rivets that fastened the lost lacing bars. In both cases, the influence of the position of the lacing bars was compared. The lost lacing bars ranged from 2–4 for the C-series cases and 2–6 for the S-series cases. The effects of the number of lacing bars lost were compared. It was assumed that the rivet was present for the cases in which rivets existed, even when the lacing bars were missing. It was assumed that the lacing bars and rivets were missing for the cases in which the rivets were missing, owing to serious corrosion.

Table 4
Investigated cases

Case name	Position of lost lacing bars	Number of lost lacing bars	Loss of rivets
N0	n/a	0	Exist
S2	Side	2	Exist
S2r	Side	2	Lost
S4	Side	4	Exist
S4r	Side	4	Lost
C2	Centre	2	Exist
C4	Centre	4	Exist
C4r	Centre	4	Lost
C6	Centre	6	Exist
C6r	Centre	6	Lost

Results

Figure 9 shows the obtained load-displacement curves. The load increased linearly by 0.8Py. The load-displacement curves were approximately identical, even for the case with missing lacing bars and rivets, except around the peak of the curves. The maximum load for each case and the corresponding reduction in loads from the normal case N0 are listed in Table 5. Figure 10 compares the maximum load and reduction, as listed in Table 5. The loss of 2–6 lacing bars reduced the maximum load by less than 2%. By contrast, the loss of the lacing bars and rivets reduced the maximum load by 5%.

Figure 11 shows the von Mises stress distribution at the maximum load. The grey range represents the yielded area. As shown in cases S4r and C6, the stress on the flange around

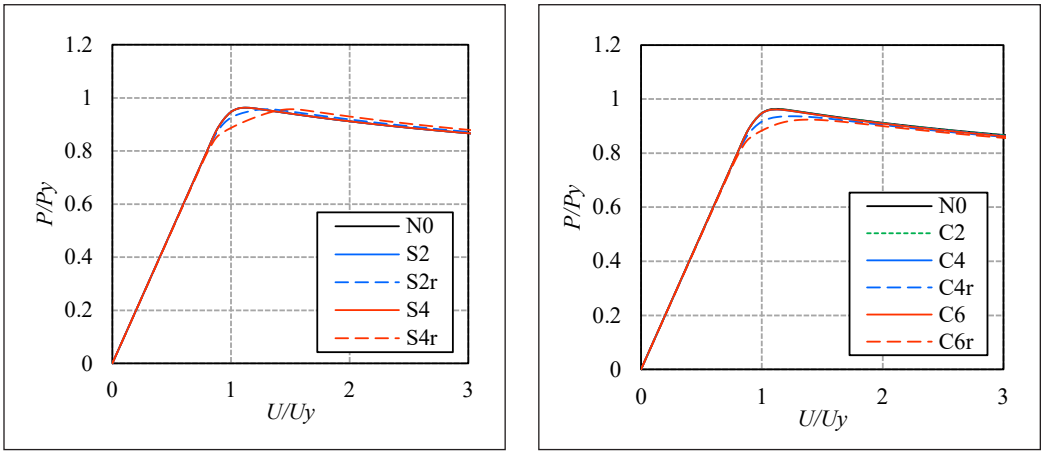

Figure 9. Load and displacement curves for the test cases. The curves of all the cases are almost the same, even when lacing bars and rivets are missing, except around the peaks: (a) Side loss cases: and (b) Centre loss cases

Table 5
Maximum load and the reduction

Case name	Maximum load [kN]	Reduction* [%]
N0	1138	0
S2	1123	-1.3
S2r	1117	-1.8
S4	1123	-1.3
S4r	1117	-1.8
C2	1122	-1.4
C4	1121	-1.5
C4r	1093	-4.0
C6	1121	-1.5
C6r	1078	-5.3

*Reduction is the percentage difference between the maximum load and the normal case N0

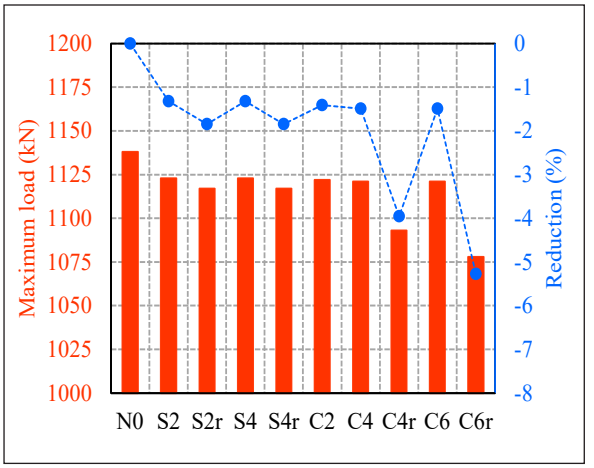

Figure 10. Maximum load for each test case. The missing of 2–6 lacing bars decreases the maximum load by less than 2%, whereas that of the lacing bars and rivets decreases the maximum load by 5%

the lost lacing bar was slightly reduced. However, for C6r, which had missing lacing bars and rivets, the stress on the flange around the lost rivet holes was significantly reduced.

Discussion

As shown in Figure 9, the loss of lacing bars or rivets did not affect the compression behaviour in the elastic range. This result suggests that the loss of lacing bars and rivets in

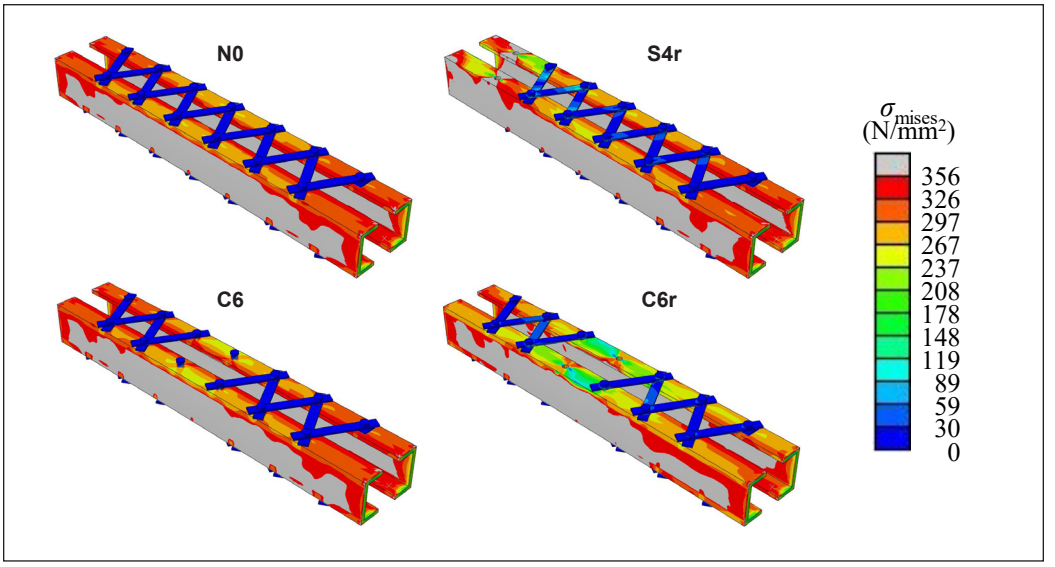

Figure 11. von Mises stress distribution at maximum load. In the cases S4r and C6, the stress on the flange around the lost lacing bar is slightly decreased. However, for C6r, which has missing lacing bars and rivets, the stress on the flange around the lost rivet holes is significantly decreased

the range investigated in this study does not affect the mechanical behaviour of the column in the service limit state. The effect of the loss of lacing bars and rivets appeared around the peak of the load beyond the elastic range, as shown in Figure 9. Therefore, the loss of the lacing bars and rivets affected the load-carrying capacity of the column. As shown in Figure 10, the loss of rivets reduced the maximum load by 5%, and the loss of only lacing bars limited the reduction of the maximum load to 2%. This is because the loss of the rivets reduced the net cross-sectional area and the compressional load transfer due to the contact between the rivet axis and hole. Although the loss of a rivet causes stress concentration around the empty rivet holes and reduces the load-carrying capacity, the bearing prevents stress concentration and reduces capacity. Hence, the loss of the rivets is an important concern when estimating the residual load-carrying capacity of built-up columns. In this study, thickness reduction due to corrosion of steel shapes was not evaluated. Because the reduction in plate thickness reduces the load-carrying capacity, the load-carrying capacity in that case should be evaluated. Because the combination of the reduction in thickness and the lacing bars causes a significant reduction in load-carrying capacity, it is necessary to evaluate that in the case where the plate thickness is reduced.

CONCLUSION

This study investigated the load-carrying capacity of built-up columns in scenarios where lacing bars and rivets were absent. Employing finite element analysis, we also examined

the critical aspect of modelling riveted connections. The ensuing results and conclusions can be summarised as follows:

The assessment of the compressional behaviour of built-up columns, achieved through finite element analysis focusing on solid elements, represents a significant departure from prior studies that predominantly relied on shell elements. The results, encompassing maximum load values, load-displacement curves, and stress distributions, demonstrated an impressive congruence between models employing solid and shell elements. This underscores the adaptability of solid elements for finite element analysis, particularly in the context of column compression, and their efficacy in facilitating intricate modelling of riveted connections.

The presence of rivet holes has an adverse effect on the load-carrying capacity of columns in compression. This is primarily attributed to the reduction in the net cross-sectional area, leading to heightened stress concentrations around the perforations. Conversely, introducing rivets to fill these holes leads to almost completely recovering the maximum load. This revival is attributed to the effective transmission of compressional forces through contact between the rivet axis and the hole. Consequently, it becomes evident that modelling the rivet and the hole is necessary for determining the behaviour of the area around the rivet connection.

The loss of 2–6 lacing bars resulted in a minimal reduction of the maximum load, typically around 2% or less. However, the absence of lacing bars combined with the presence of filled rivets caused a more substantial reduction in the maximum load, peaking at 5%. This phenomenon can be ascribed to the absence of rivets, which not only diminishes the net cross-sectional area but also disrupts the transfer of compressive loads through the loss of contact between the rivet axis and the hole, thus promoting stress concentration around the hole. Consequently, the presence or absence of rivets is a pivotal consideration in estimating the residual load-carrying capacity of built-up columns.

ACKNOWLEDGEMENT

This work was supported by JSPS KAKENHI Grant Number JP19K04587.

REFERENCES

Beaulieu, L. V., Legeron, F., & Langlois, S. (2010). Compression strength of corroded steel angle members. *Journal of Constructional Steel Research*, *66*, 1366–1373. https://doi.org/10.1016/j.jcsr.2010.05.006

Hisazumi, K., Kanno, R., & Tominaga, T. (2018). Local buckling behavior and strength evaluation of corroded steel shapes. *Steel Construction Engineering*, *25*(99), 67–76. https://doi.org/10.11273/jssc.25.99_67

Iwatsubo, K., Oda, N., Miyoshi, T., Takai, T., & Tamada, K. (2020a, September 7-9). *The design and the ultimate strength behavior of built-up columns subjecting the compressive load*. [Paper presentation]. Proceedings of Japan Society of Civil Engineers Annual Meeting, Tokyo, Japan

Iwatsubo, K., Oda, N., Miyoshi, T., Takai, T. & Tamada, K. (2020b). The strength behavior of the built-up columns used the channel members. *Proceedings of Constructional Steel, 28,* 102–108.

JIS G 3106 (2020). *Rolled steels for welded structure*. Japanese Industrial Standards. chrome-extension://efaidnbmnnnibpcajpcglclefindmkaj/https://webdesk.jsa.or.jp/preview/pre_jis_g_03106_000_000_2020_e_ed10_ch.pdf

JRA (1980). *Specifications for Highway Bridges*. Japan Road Association.

JRA (1990). *Specifications for Highway Bridges*. Japan Road Association.

Kojima, Y., Takai, T. (2021). Fundamental investigation on buckling eigen value of built-up column considering initial imperfection. *Japan Society of Civil Engineers, I-026*, 51–52.

Miyoshi, T. (2021a). Investigation on strength provisions of built-up column in design standards for Japanese highway bridges. *Memoirs of National Institute of Technology, 63*, 1–8.

Miyoshi, T., Iwatsubo, K., Takai, T. & Tamada, K. (2021b, September 6-10). *Material properties of a steel truss bridge built-up member passing 115 years since the completion*. [Paper presentation]. Proceedings of Japan Society of Civil Engineers Annual Meeting, Tokyo, Japan

Miyoshi, T., Iwatsubo, K., Takai, T. & Tamada, K. (2021c). Material properties of a steel bridge built-up member passing 115 years since the completion. *Proceedings of Constructional Steel*. *29*, 48–57.

Miyoshi, T., Nakakita, T., Iwatsubo, K., Takai, T. & Tamada, K. (2022). Compression strength of aged built-up column with vanished lacing bars. In A. Zingoni (Ed.) *Proceedings of the 8th International Conference on Structural Engineering, Mechanics and Computation* (pp. 950–955). CRC Press.

Nakakita, T., Miyoshi, T., Iwatsubo, K., Takai, T., Satake, R. & Tamada, K. (2021, September 6-10). *Residual stress distribution of a steel truss bridge built-up member passing 115 years since the completion*. [Paper presentation]. Proceedings of Japan Society of Civil Engineers Annual Meeting, Tokyo, Japan.

Nakakita, T., Miyoshi, T., Iwatsubo, K., Takai, T., & Tamada K. (2022). Investigation on residual stress of an aged channel-shaped steel and compression strength of a built-up column with disappeared lacing bars. *Journal of Structural Engineering A*, *68A,* 112–122. https://doi.org/10.11532/structcivil.68A.112

Paik, J. K., Lee, J. M., & Ko, M. J. (2004). Ultimate shear strength of plate elements with pit corrosion wastage. *Thin-Walled Structures*, *42*(8), 1161–1176. https://doi.org/10.1016/j.tws.2004.03.024

Sadovsky, Z., & Drdacky, M. (2001). Buckling of plate strip subjected to localised corrosion—A stochastic model. *Thin-Walled Structures*, *39*(3), 247–259. https://doi.org/10.1016/S0263-8231(00)00060-4